

---

# Analysis of a Possible Coupling in a Thrust Inverter

**Raphael Lardat\*** — **Bruno Koobus\*\*** — **Eric Schall\*\*\***  
**Alain Dervieux\*** — **Charbel Farhat\*\*\*\***

\* INRIA, 2003 Route des Lucioles, F-06902 Sophia-Antipolis Cedex,  
Raphael.Lardat@Inria.fr, Alain.Dervieux@Inria.fr

\*\* Université de Montpellier II, Place Eugène Bataillon, Département de  
Mathématiques, CC 051, F-34095 Montpellier Cedex 5 and INRIA,  
koobus@math.univ-montp2.fr

\*\*\* Université de Pau, IUT Génie Thermique et Energétique, 1, Avenue de l'Université,  
F-64000 PAU, Eric.Schall@univ-pau.fr

\*\*\*\* University of Colorado at Boulder, Campus Box 429, Dept. of Aerospace Eng.  
Sciences, Boulder, Colorado 80309-0429, U.S.A, charbel@boulder.colorado.edu

---

*ABSTRACT. We present the study of the interaction between the flow in a thrust inverter and a flap playing a central role in the flow deviation. The flow is limited by a rather closed vessel and presents acoustic modes which can be amplified by recirculations. Such modes may interfere with structural modes. The analysis is conducted with a fully ALE 3D approach involving a nonlinear compressible flow solver, coupled with a shell finite element model.*

*RÉSUMÉ. Nous présentons l'étude d'une interaction entre l'écoulement dans un inverseur de poussée et un volet jouant un rôle central dans la déviation de l'écoulement. Cet écoulement est délimité par une enceinte partiellement close et présente des modes acoustiques susceptibles d'être amplifiés par leur couplage avec des recirculations. De tels modes peuvent interférer avec certains modes de la structure du volet. L'analyse de ce phénomène est réalisée à l'aide d'une méthode numérique 3D en formulation eulérienne-lagrangienne, couplant un modèle compressible non linéaire pour l'écoulement avec un modèle en éléments finis de type coque pour la structure.*

*KEYWORDS: fluid/structure interaction, Arbitrary-Lagrangian-Eulerian formulation, thrust inverter, Euler equations.*

*MOTS-CLÉS: interaction fluide/structure, formulation d' Euler-Lagrange-Arbitraire, inverseur de poussée, équations d'Euler.*

---

## 1. Introduction

Thrust inverters are a crucial device for the reduction of landing distances for commercial aircrafts. They involve complex mechanisms: they have to be completely inoperative on the engine flow in any part of the travel except landing; then several pieces have to move in order to allow an efficient deviation of this flow, forcing it to go forward instead of backward. We are therefore talking about a device that is made of several moving pieces, that should strongly act on the engine flow. Further more, the considered flow is rather confined in a partly closed box of complex geometry, which results in acoustic phenomena and large recirculations. A significant part of the jet deviation is caused by a flap which endures large forces from the flow. The motivation of our study is to investigate which kind of mechanical coupling can arise in the case of under-dimensioned design of this flap.

For this preliminary study, several geometrical and physical simplifications are introduced. The modelization and software involve a finite-element dynamical shell model for the structure, and a finite-element finite volume upwind Euler model for the flow. Coupling between both models is built through a full ALE formulation for the fluid, and proper transmission of efforts through a non-conforming discrete interface [FAR 98]. Special care has been paid to space-time integration, (see [FAR 95]).

The purpose of the present paper is to give a first glance of mechanical issues involved in the fluid-structure interaction, and to analyse the numerical questions related to their accurate prediction by the proposed methods.

Many fluid-structure interaction systems have been studied and calculated with various methods. However, the present problem does not seem having been studied in the litterature. Restricting to compressible flows, and to unstable coupling, we would say that most contributions have focused on aerodynamic flutter at different regimes (see for example [FAR 95]). In that case, the unstable mode is a structural one whose energy is feeded by the flow, that would be steady in the case of an infinitely stiff structure.

In some other context, the flow itself has intrinsic fluctuation mode. This is the case when vortex shedding can influence some "receptor" such as an aircraft fin, or the edge of a bridge [TRA 98], or the outlet of a rocket [CAR 98], [CAR 99]. Such flow configurations are difficult to simulate since they require a sophisticated viscous flow model (e.g. Reynolds Averaged Navier-Stokes) and therefore a large computing effort. In the case of purely acoustic pulsation, the flow model can be much simplified and a non-linear model is not necessary. In the present case, acoustic pulsation has its influence increased by its effect on a recirculation. Therefore a non-linear flow model is compulsory.

The plan of the paper is as follows:

We start by a short overview of the numerical model; then, the investigation of the uncoupled flow is considered, followed by a description of the structural model and of

its main eigen modes. Finally, the paper presents a simulation of a coupled unstable phenomenon.

## 2. About numerical model

### 2.1. Generic properties

The numerical tool is exactly the same as the one used in the brother papers in this issue [SCH 99] and [LAR 00]. In short, it relies on an unsteady three-field model consisting of a structural model (a shell), a fluid model (compressible Reynolds-Averaged Navier-Stokes), a pseudo-elasticity model for the dynamical fluid mesh. It is useful for the sequel to present the system describing the coupled model:

$$\begin{aligned} \frac{\partial}{\partial t}(V(x, t)W(t)) + F^c(W(t), x, \dot{x}) &= R(W(t), x) \\ M \frac{\partial^2 q}{\partial t^2} + f^{int}(q) &= f^{ext}(W(t), x) \\ \tilde{M} \frac{\partial^2 x}{\partial t^2} + \tilde{D} \frac{\partial x}{\partial t} + \tilde{K} x &= K_c q \end{aligned} \quad [1]$$

where  $t$  designates time,  $x$  the position of a moving fluid grid point,  $W$  is the fluid state vector,  $V$  results from the finite element/volume discretization of the fluid equations,  $F^c$  is the vector of convective ALE fluxes,  $R$  is the vector of diffusive fluxes,  $q$  is the structural displacement vector,  $f^{int}$  denotes the vector of internal forces in the structure,  $f^{ext}$  the vector of external forces,  $M$  is the finite element mass matrix of the structure,  $\tilde{M}$ ,  $\tilde{D}$  and  $\tilde{K}$  are fictitious mass, damping and stiffness matrices associated with the moving fluid grid and  $K_c$  is a transfer matrix that describes the action of the motion of the structural side of the fluid/structure interface on the fluid dynamic mesh.

An implicit time advance finite-element scheme is used for the structural model and an implicit time advance, time-staggered with respect to structure, vertex-centered upwind finite volume scheme is used for the fluid part.

### 2.2. Specific options

Although the flow is supersonic in some part, the shock capturing facilities in the fluid model are inhibited (“no limiter”) because we do not expect shocks. Moreover, since recirculation is important, a low level of numerical dissipation is mandatory. For this purpose, a scalar coefficient  $\gamma$  is used to weight the numerical viscosity introduced by the Roe approximate Riemann solver. This new scheme called  $\beta - \gamma$  and described in [CAR 99], reads:

$$\begin{aligned} Flux(W_L, W_R, \vec{n}) &= 0.5 (Flux(W_L, W_L, \vec{n}) + Flux(W_R, W_R, \vec{n})) \\ &- 0.5 \gamma |J|(W_L - W_R) \end{aligned} \quad [2]$$

in which L stands for left, R for right,  $\vec{n}$  is the normal vector to cell boundary and  $J$  the scalar product of the Jacobian of fluxes with the normal vector  $\vec{n}$ . Usual option

is  $\gamma = 1$  for standard Roe solver and for lower values of numerical viscosity, smaller values of  $\gamma$  will be preferred.

The choice of in/out boundary conditions was *a priori* a sensitive one. Indeed, the geometrical domain was initially exactly restricted to the inverter cavity and we decided to generate a larger domain in order to insure that domain truncation did not carry large unaccuracies.

Moreover, due to the mixed supersonic-subsonic character of the outlet, which may also involve incoming flow, we had to derived a new form of the Steger and Warming boundary condition. The numerical flux on a node  $i$  located at the outlet boundary reads:

$$J^+(W_i)W_i + J^-(W_i)W_\infty$$

whith  $J = J^+ + J^-$  and where  $J^+$  and  $J^-$  represent the matrices using respectively the positive and negative eigen values of the Jacobian of fluxes,  $W_i$  the fluid state vector on the boundary node  $i$  and  $W_\infty$  the imposed farfield state vector. The expected weak dependancy on geometrical truncation was obtained thanks to an adhoc choice of the farfield state vector:

$$\text{if } \vec{v} \cdot \vec{n} > 0 \text{ then } W_\infty = \begin{pmatrix} \rho_i \\ \rho_i u_i \\ \rho_i v_i \\ \rho_i w_i \\ \frac{p_{out}}{\gamma-1} + \frac{1}{2} \rho_i V_i^2 \end{pmatrix} \text{ else } W_\infty = \begin{pmatrix} \rho_{out} \\ 0 \\ 0 \\ 0 \\ \frac{p_{out}}{\gamma-1} \end{pmatrix}$$

where  $\vec{v}$  is the velocity vector,  $\vec{n}$  the outgoing boundary normal vector,  $\rho_{out}$  and  $p_{out}$  respectively the farfield density and pressure.

### 3. Main features of the flow

This section aims at giving a few information about the flow topology before its coupling with the structure.

#### 3.1. Definition of the geometry

A thrust inverter is located in the last part of an aircraft turbo-engine. In cruise or in take off regime, it should let the flow go towards the rear outlet. To create the thrust inverter, several parts of the engine are moved. Mainly, a quasi-rectangular door is opened in the flow duct; in its rotation, it will essentially shut the path towards the outlet. When hitting this door, the flow is forced to change its direction and goes away from the engine axis. At last, a flap fixed orthogonally to the door will make the flow go backward with respect to its initial direction (see Figure 1). A second fixed rigid flap prolongates the upper part of the inlet vessel.

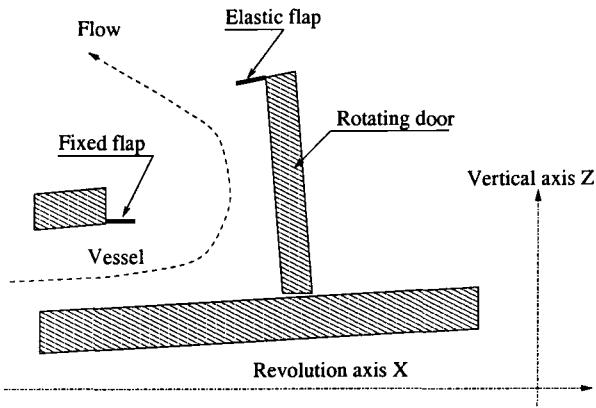


**Figure 1.** *Sketch of the thrust inverter geometry*

The computational domain is restricted to one portion of the thrust inverter, i.e. only an angular fraction of the vessel will be computed. Nevertheless, this geometrical domain contains one rotating door in its globality.

The skin of the global fluid mesh is depicted in Figure 2: we see an angular section of the annular incoming flow (bottom of mesh), the vertical section corresponds to the thickness between the engine duct and the external atmosphere. The upper part is an arbitrary truncation of the external medium. The solid walls are depicted in Figure 3 : the axial duct is to be seen at the forefront; the vertical rotated door is visible in the upper part of the image and inside the duct; it does not completely shut the axial duct as shown by the “white hole”. The upper plan of this mesh shows a strong local refinement; this supports the elastic flap, apparently fixed on the inverter door, producing the second deviation of the flow. This flap will be flexible and will be the object of the aeroelasticity study. The global fluid mesh is rather coarse for a complex 3D geometry and is made of 192535 tetrahedra and 35645 nodes.

### 3.2. Numerical flow behavior

The inlet flow is subsonic with a Mach number of 0.8, the expansion rate of 1.5 produces an outlet flow with supersonic zones. Taking care of the artificial outlet boundary condition (described in section 2.2), the numerical simulation gives a quasi-periodic flow (195 Hz) with vortex shedding starting from the fixed flap prolongating the axial duct. This shedding is coupled to a pressure fluctuation in the whole vessel.

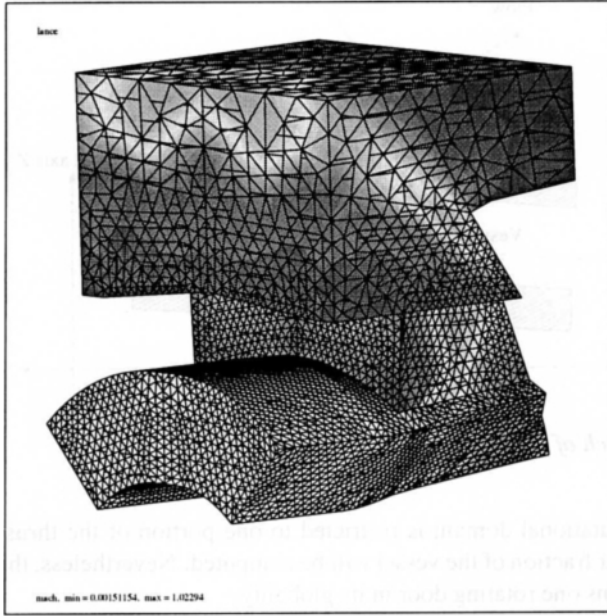


**Figure 2.** Complete fluid mesh skin; Mach number

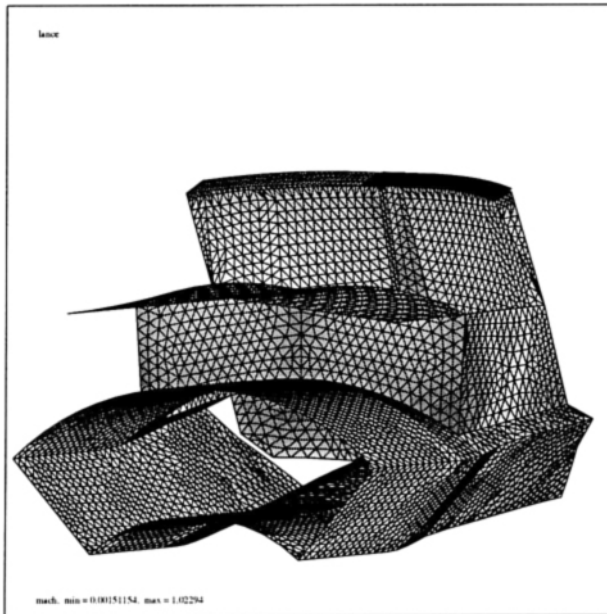


**Figure 3.** Solid walls; Mach number

This behaviour is illustrated in Figures 4 to 6 where times (a) and (b) correspond respectively to the minimum and maximum of the efforts on the flap. At time (b), a vortex is located in front of the elastic flap, reducing the cross-section of the jet which increases the pressure on the flap but reduces the pressure at the bottom of the vessel. On the other hand, at time (a), the cross-section of the jet is larger and the pressure is lowered on the flap and increased at the bottom of the vessel.

To obtain this result with this rather coarse mesh, the internal viscosity of the spatial scheme had to be reduced by a factor two, by tuning the parameter multiplying the artificial viscosity term in the approximate Roe-type Riemann solver ( $\gamma = 0.5$  in Eq. 2). This was possible because the flow, although transonic, does not involve any shock. When using the usual (twice larger) internal viscosity, the frequency of the flow is moved to 180 Hz and the amplitude is strongly reduced. In this case, the flow is quasi-steady, with no vortex shedding and the forces fluctuations on the elastic flap seem to be caused by purely acoustic modes.

A third attempt to reduce further the viscosity (by a factor four with respect to standard) has not produced a solution. At this stage, we feel a few comments are needed to a better understanding of this partly enclosed flow:

- The small difference between the two frequencies 180 and 195 Hz (only 8% change) seems to prove that acoustic is the key factor responsible for the choice of the flow frequency even in the case of vortex shedding. According to our previous experience of internal flows, the frequency of the vortex shedding produced by an Euler model and a singular geometry is set by predominant reflective acoustic modes. Note that, in this specific case, the length between the flap and the bottom of the duct is roughly 0.9 meter which is leading to an acoustic frequency of about 185 Hz.

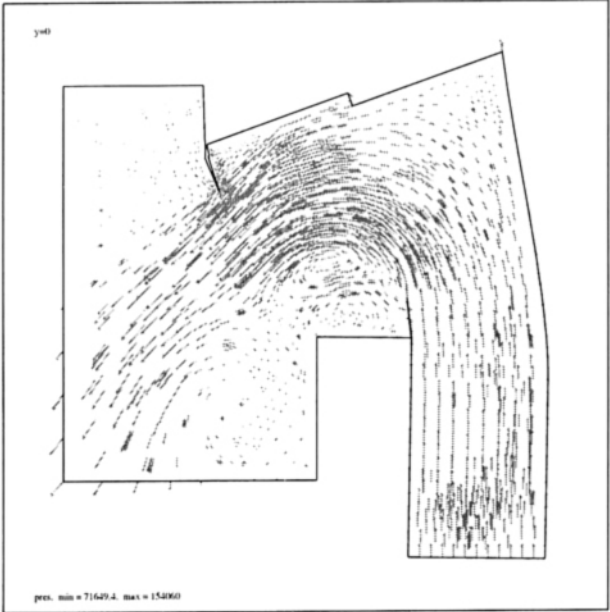
- Decreasing the numerical viscosity has nevertheless an action on the flow frequency which corresponds to the influence, weaker but not negligible, of the dissipative effects produced by the numerical model.

#### 4. Structural modes

The flap is a structure located at the end of the mobile door and has a quasi rectangular shape. It is modelled by shell elements with a mesh involving  $5 \times 73 = 365$  nodes and 576 triangles. The thickness of the shell elements is variable, smaller at the edge and thicker near the door.

Due to the fact that this flap is a mobile piece, it is not fixed to the door, but held by a rod so that: at both extremities, translations are not possible. At its middle it is held so that vertical translations are not possible. Rotations are possible around  $y$  axis at middle and extremities. With these conditions, the first six modes correspond to the following frequencies:

Mode	1	2	3	4	5	6
Frequency (Hz)	181	210	319	508	654	676



(a)

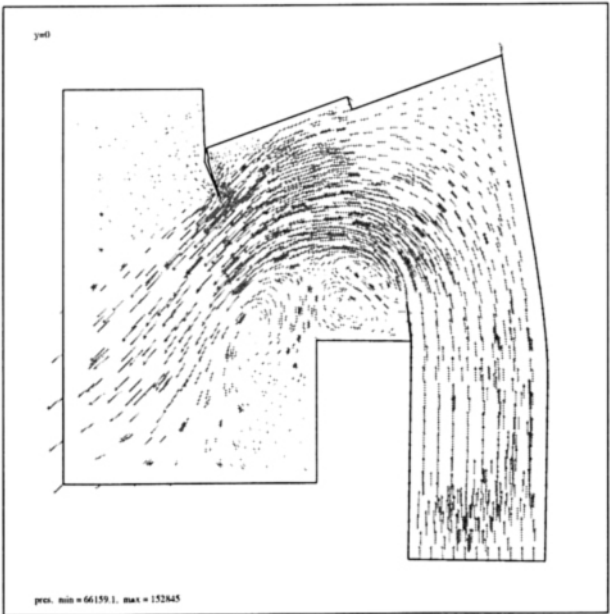
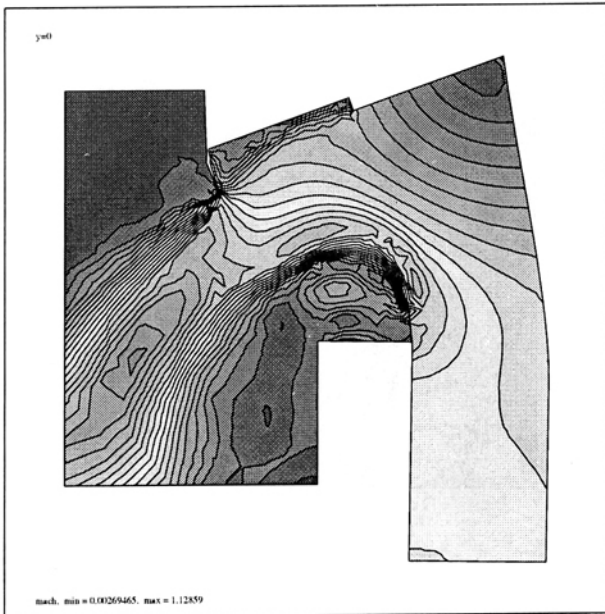


**Figure 4.** Section at symmetry plane  $y = 0$ , velocity field for times (a) and (b)



(a)

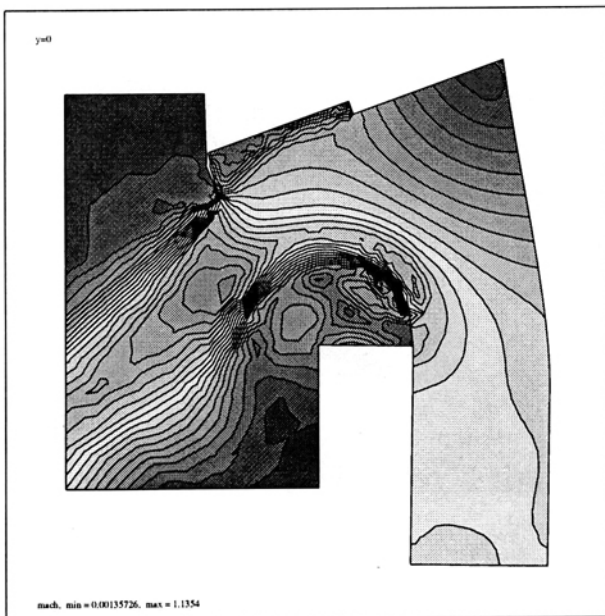
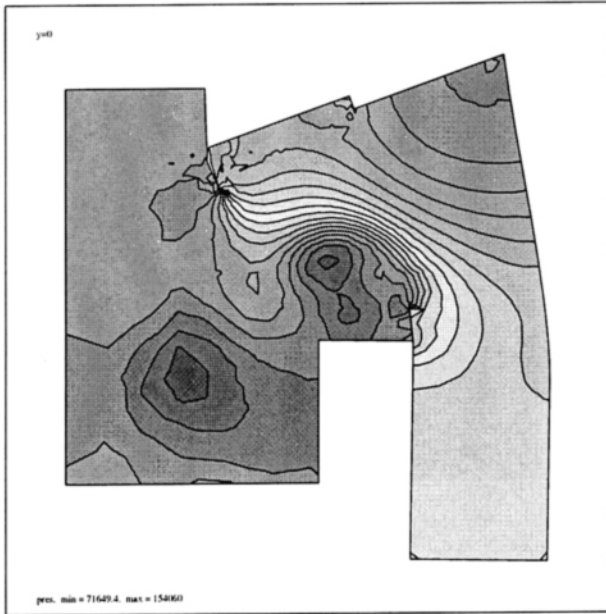


**Figure 5.** Section at symmetry plane  $y = 0$ , Mach number for times (a) and (b)



(a)

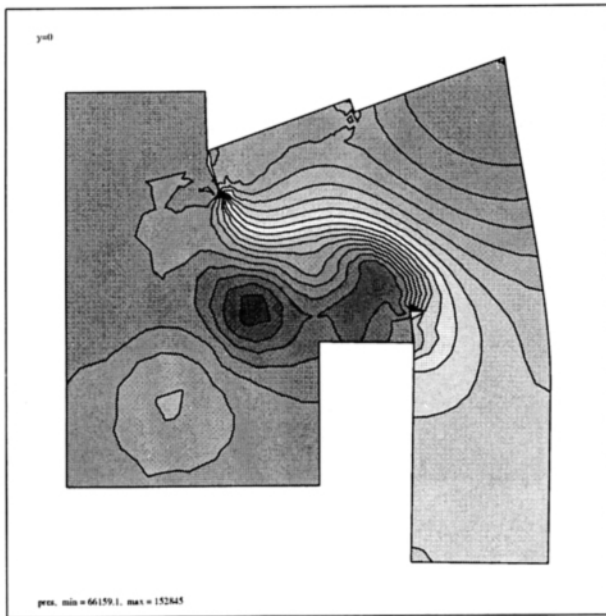
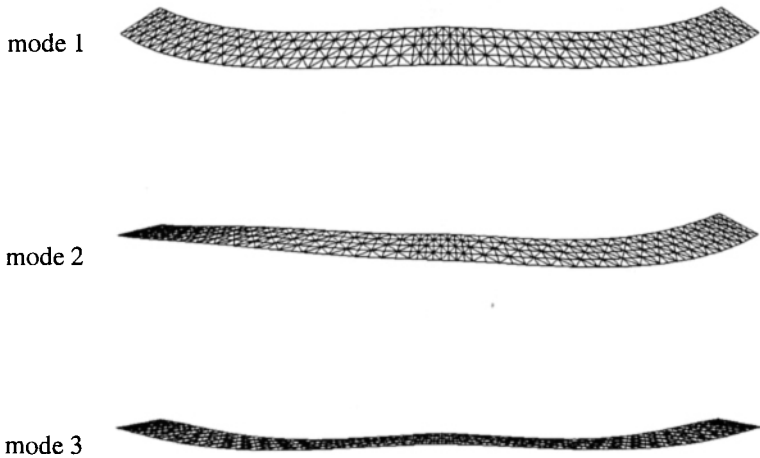


Figure 6. Section at symmetry plane  $y = 0$ , pressure field for times (a) and (b)



**Figure 7.** *View of the three first modes of the flap*

We propose a few pictures of these modes in Figure 7; it seems that the first mode is of torsion type (around  $y$  axis), the second mode is not symmetrical with respect to symmetrical plane  $y = 0$ , the third one seems of flexion type.

We observe that the first frequency (181 Hz) is not so different from the fluid frequency (195 Hz).

## 5. Static effects

First, a computation of the static coupling is performed by introducing a damping matrix in the unsteady shell model. A result (steady structure) is obtained in 50 iterations. Surprisingly, the largest displacement arises at the rear part of the flap, near the door, since the edge of the flap rotates against flow, the rear part rotates in the flow direction, just as the flap would be inflated by the flow. We have verified that this is explained by larger values of the static pressure at the rear part of the flap. In particular, in a more realistic geometry, this deformation would induce some loss of fluid and pressure through the hole provoked by the deviation between the flap and the door. In Figure 8 we try to give an idea of the flap deformation.

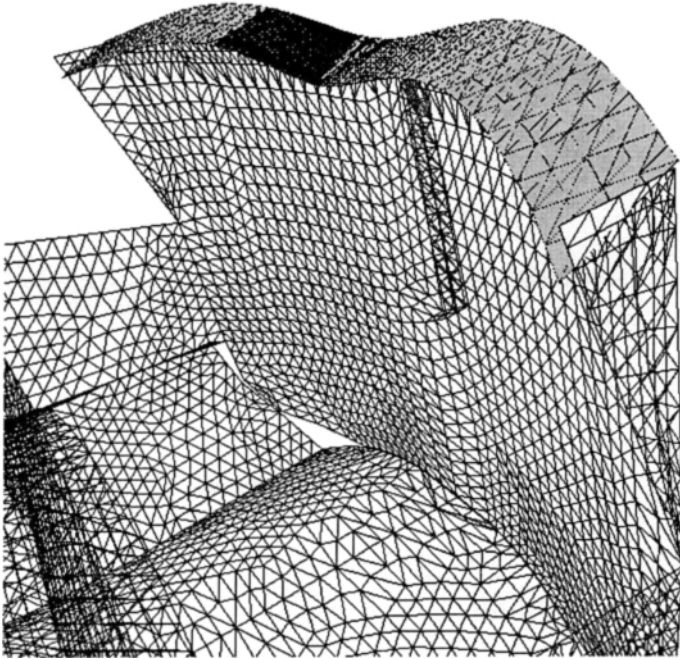


**Figure 8.** *The static flap deformation : grey part at top, the flap mesh, else, the inverter walls; amplification of deformation by 32*

## 6. Unsteady coupling

We start the coupled solution, with the static deformation as initial solution (mesh deformation, shell displacement, previously computed flow), but this time, we set the structure damping to zero. The unsteady calculation is applied with second-order accuracy in time. After some transient, we obtain a motion of the structure with a rather large amplitude, see Figures 10 and 11, which shows that, despite the difference of frequencies, the structural first mode is well excited by the fluid pulsation. We observe no long term tendency to amplify or damp. In fact, we detect a clear beating in Figures 9, 10 and 11, with an amplitude frequency of about 14 Hz, in a good agreement with the difference 195-181 between the two pure frequencies of fluid and structure. One should also note that the aerodynamical forces  $C_x$  and  $C_z$ , see Figures 12, 13, are in phase opposition with respect to the vertical displacement of the structure. It seems to lead to a stabilized amplitude of motion: an increase of the displacement lower the force and on the contrary, a decrease of the displacement raise the force. It can be seen as: when the structure is set into motion, the structure and the flow are in phase which automatically reduces the force applied by the flow over the structure. This propriety make us believe that, with an Euler model and even in the case where the frequency of the first structure mode is equal to the fluid frequency, there will be no flutter.

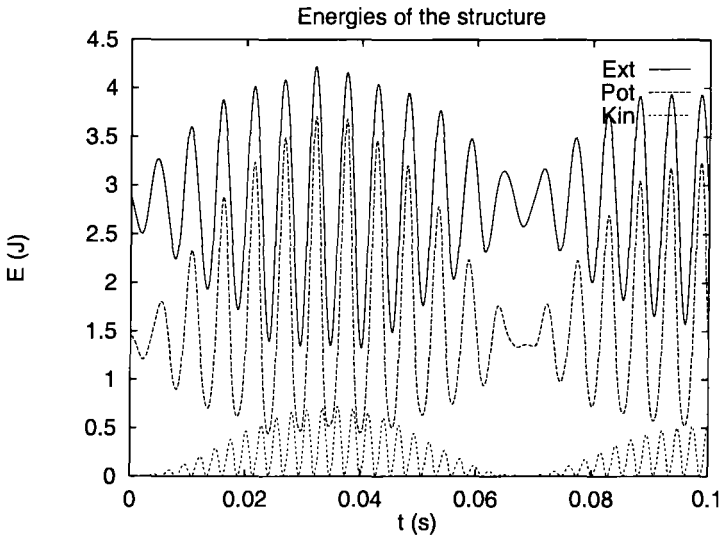


**Figure 9.** Structure's energies (potential, external and kinetic)

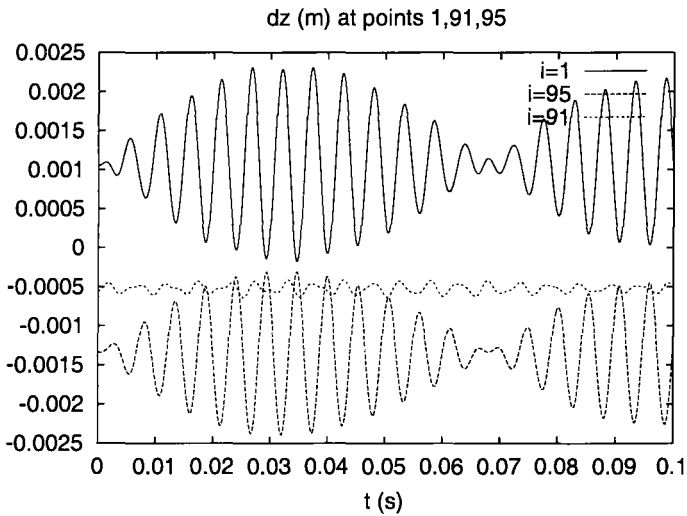


**Figure 10.** Vertical displacement ( $z$ ) of a sample of structure's points

Indeed, the flutter phenomenon can be characterized by the chain: amplification of deformation  $\Rightarrow$  amplification of force  $\Rightarrow$  amplification of deformation.

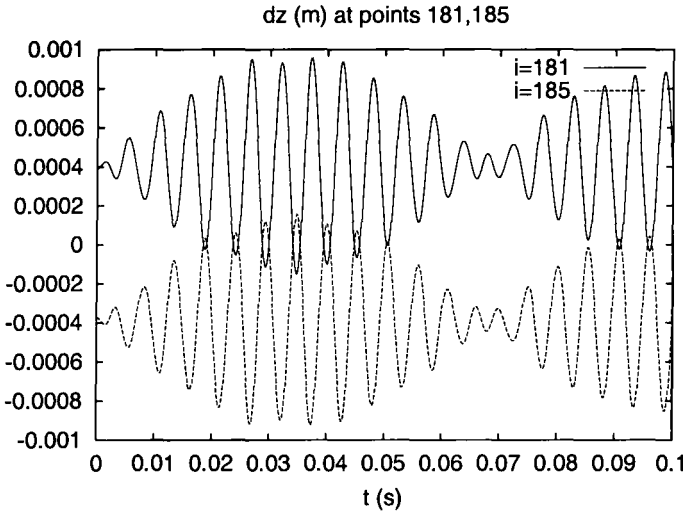


Figure 11. Vertical displacement ( $z$ ) of a sample of structure's points (end'd)

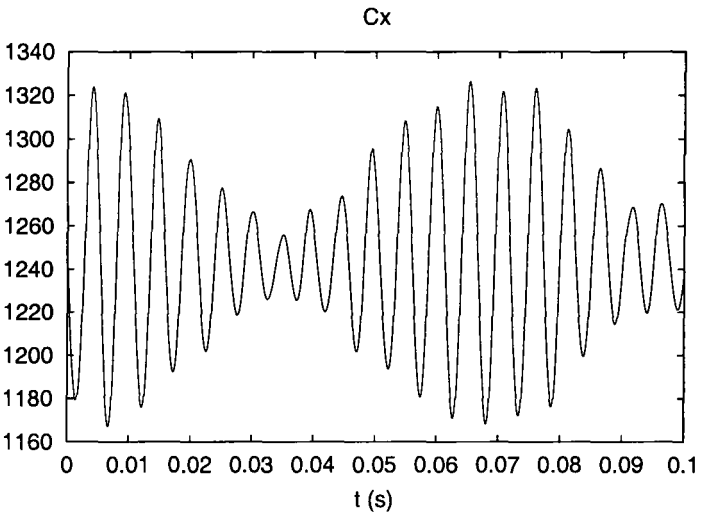
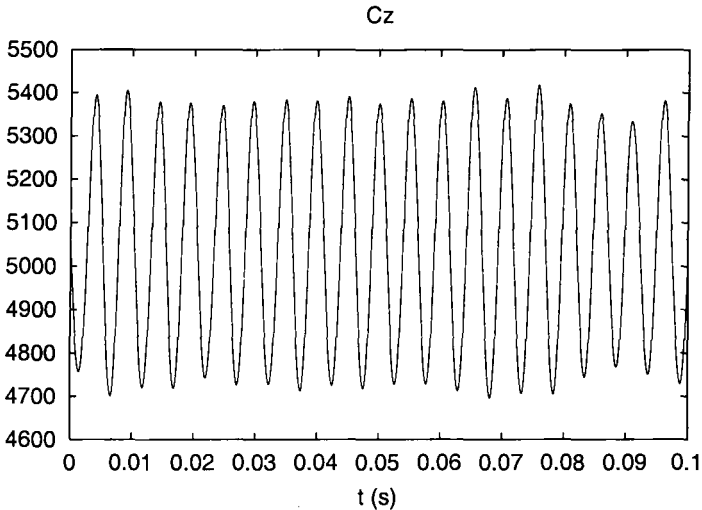


Figure 12. Aerodynamical force  $C_x$



**Figure 13.** Aerodynamical force  $C_z$

## 7. Conclusion

To sum up this paper, we have applied a complex non-linear tool involving a sophisticated CFD solver to the investigation of the possible fluid-structure coupling in the thrust inverter of a jet engine. The main advantage of this approach is its accurate description of the geometry. The numerical model of the flow has been the object of a particular investigation. Indeed, an unsteady non-linear conservative model of Euler type is used in a computational domain that is geometrically well described, thanks to the use of an unstructured-mesh approach. Further more, the domain size influence and the numerical viscosity influence have been examined. Taking care of this, the simulation has been able to detect an intrinsic flow fluctuation, combining acoustic phenomena and recirculation. The recirculation is induced by a sudden enlargement and a singularity point located at the end of the fixed flap. We assume that the resulting vortex shedding can be simulated by an inviscid model. Indeed we believe that the recirculation frequency and size will not be much influenced by friction phenomena but rather by coupling with acoustics. Another example of such aeroacoustic coupling involving vortices that can be accurately predicted with an unsteady conservative Euler model is the aeroacoustic coupling in a rocket powder propulsor ([CAR 98] and see paper [LAR 00] in this issue). It is necessary to point out that the flexible flap may be a second source of vortex shedding. However, this vortex shedding could not be obtained with our coarse mesh. Moreover, it would arise in a rather external part of the flow and would not be necessarily well constrained by acoustics and thus an Euler model would be more questionable. The coupling between the aeroacoustic pulsation and the first mode of the structure has been put in evidence and explained. Up to now we can reclaim only a qualitative sound of our study. Comparison with experiments

would bring a new light on the phenomenon and especially the validation of the flow prediction. In that case, unsteady calculations will be very useful for producing *a priori* estimates concerning the confidence interval for parameters in order to avoid fluid-structure coupled oscillations, that can induce noise or early weariness. Improvements in prediction could be investigated by applying turbulence modelling (RANS or LES), as far as measurements would be available for validation and calibration. The challenge for this application is indeed to compute with fine enough meshes.

#### Acknowledgements

The authors acknowledge the support and the technical informations given by Hispano-Suiza at Le Havre and the access to the Origin 2000 computer provided by Centre Charles Hermite at Nancy.

#### 8. References

- [SCH 99] SCHALL E., LARDAT R., DERVIEUX A., KOOBUS B., FARHAT C., "Investigation of the Aeroelastic Coupling between a Nozzle and a Supersonic Jet", *this issue*.
- [CAR 99] CARPENTIER R., "Le schéma  $\beta - \gamma$  en axisymétrique", *INRIA research report* 3676, 1999
- [CAR 98] CARPENTIER R., HULIN A., "Numerical Unstable Modes in Unsteady Simulations of Natural Vortex Shedding" *Pressure Vessels and Piping Conference*, ASME/JSME, San Diego, July 26-30, 1998
- [GUI 98] GUILLARD H., VIOZAT C., "On the Behaviour of Upwind Schemes in the Low Mach Number Limit", *Comput. Fluids* 28, 1998, pp. 63-86.
- [FAR 95] FARHAT C., "High Performance Simulation of Coupled non-linear Transient Aeroelastic Problems", *AGARD Report R-807*, Special Course on Parallel Computing in CFD (l'Aérodynamique numérique et le calcul en parallèle, North Atlantic Treaty Organization (NATO), October 1995.
- [FAR 98] FARHAT C., LESOINNE M. AND LE TALLEC P., "Load and Motion Transfer Algorithms for Fluid/Structure Interaction problems with Non-Matching Discrete Interfaces: Momentum and Energy Conservation, Optimal Discretization and Application to Aeroelasticity", *Computer Methods in Applied Mechanics and Engineering*, Vol. 157, pp. 95-114, 1998.
- [LAR 00] LARDAT R., CARPENTIER R., KOOBUS B., SCHALL E., DERVIEUX A., FARHAT C., GUERY J.-F. AND DELLA PIETA P., "Interaction Between a pulsating flow and a perforated membrane", *this issue*.
- [TRA 98] TRAN H., KOOBUS B. AND FARHAT C., "Numerical Simulation of Vortex Shedding Flows Past Moving Obstacles Using the  $k-\epsilon$  Turbulence Model on Unstructured Dynamic Meshes", *La Revue Européenne des Eléments Finis*, Vol. 6, 5/6, pp. 611-642, 1998.